JMB

Available online at www.sciencedirect.com

ScienceDirect

ELSEVIER

Periodic Forces Trigger a Complex Mechanical Response in Ubiquitin

Piotr Szymczak[1] and Harald Janovjak[2]*

[1]*Institute of Theoretical Physics, Warsaw University, Hoza 69, Warsaw 00-681, Poland*

[2]*Department of Molecular and Cell Biology, University of California at Berkeley, 279 Life Sciences Addition, Berkeley, CA 94720, USA*

Edited by D. Case

Mechanical forces govern physiological processes in all living organisms. Many cellular forces, for example, those generated in cyclic conformational changes of biological machines, have repetitive components. In apparent contrast, little is known about how dynamic protein structures respond to periodic mechanical information. Ubiquitin is a small protein found in all eukaryotes. We developed molecular dynamics simulations to unfold single and multimeric ubiquitins with periodic forces. By using a coarse-grained representation, we were able to model forces with periods about 2 orders of magnitude longer than the protein's relaxation time. We found that even a moderate periodic force weakened the protein and shifted its unfolding pathways in a frequency- and amplitude-dependent manner. A complex dynamic response with secondary structure refolding and an increasing importance of local interactions was revealed. Importantly, repetitive forces with broadly distributed frequencies elicited very similar molecular responses compared to fixed-frequency forces. When testing the influence of pulling geometry on ubiquitin's mechanical stability, it was found that the linkage involved in the mechanical degradation of cellular proteins renders the protein remarkably insensitive to periodic forces. We also devised a complementary kinetic energy landscape model that traces these observations and explains periodic-force, single-molecule measurements. In turn, this analytical model is capable of predicting dynamic protein responses. These results provide new insights into ubiquitin mechanics and a potential mechanical role during protein degradation, as well as first frameworks for dynamic protein stability and the modeling of repetitive mechanical processes.

Introduction

Mechanical forces drive essential cellular processes such as the synthesis, import, and degradation of proteins;[1–4] packaging and replication of nucleic acids;[5–7] cytoskeleton organization;[8–11] and mechano-signaling.[12,13] In a majority of these functions, forces are actively generated by biological machines, such as the ubiquitous motor family of ATPases associated with diverse cellular activities (AAA-ATPases).[8,14] AAA-ATPases and other biological motors transform chemical energy into directed motions *via* nucleotide-hydrolysis-mediated conformational changes.[6,14,15] As a direct consequence of these chemo-mechanical cycles, biological machines are repetitive force generators, and it is believed that forces with periodic signatures are experienced by biomolecules in many physiological contexts.[16–23] For instance, it has been postulated that an ATP-dependent 'pulling' force is utilized by proteasomes and mitochondrial import machines to unfold proteins.[16,18,24–26] Similarly, optical trapping experiments revealed that the force generated by the motor protein dynein is oscillatory.[20]

These broad roles of repetitive mechanical forces contrast sharply with the scarcity of knowledge on the response of protein structures to this unique mechanical perturbation. Theoretical accounts on periodic biomechanics were reported as early as two decades ago.[27] This work lay dormant for

Corresponding author. E-mail address: harald@berkeley.edu.

Abbreviations used: MD, molecular dynamics; CV, constant velocity; F–D, force–displacement.

many years, likely because of the absence of mechanical, single-molecule measurements and molecular computer simulations. More recently, several groups included periodic forces in numerical models of receptor–ligand bonds and enzyme kinetics.[28–31] They found optimal ranges of force frequency and amplitude that accelerate bond breakage or product formation. However, these kinetic models built on energy landscapes determined in non-periodic experiments and did not include dynamic protein structures. Fundamental questions thus still remain: How do protein structures respond to periodic forces of different frequencies and amplitudes? Can periodic forces shift reaction pathways or modulate energy landscapes of proteins? Do these effects occur on scales that are relevant in the context of forces generated by biological machines?

Direct measurements of the nano-mechanics of biomolecules, for example, with experimental force probe techniques[32] or molecular dynamics (MD) and Monte Carlo simulations[33], have been revolutionizing the way we answer biomechanical as well as biochemical questions.[34] Efforts have been focused on proteins with known or anticipated biomechanical functions, such as immunoglobulin domains from giant muscle proteins[35] or ubiquitin.[36] The highly conserved, 76-amino-acid-long protein ubiquitin serves as a cellular signaling tag in all eukaryotic cells.[37] Ubiquitin targets proteins to different reaction pathways, and substrates destined for degradation at the proteasome are covalently modified with multimeric ubiquitin chains.[38] It is well known that proteasome–ubiquitin contacts are essential in substrate recognition. However, the role of these contacts and ubiquitin's stability during substrate unfolding is much less understood.[39,40] This potential biomechanical role of ubiquitin motivated several groups to dissect its biomechanics in force probe experiments[39,41–44] and simulations.[45–52] These studies also initiated a vivid discussion of ubiquitin's (un)folding pathways.[53] At about the same time, instrumentation was developed to apply periodic forces to single molecules,[54,55] but the molecular mechanisms underlying the measured dynamics of diverse proteins remained largely unexplained.[56–60]

We systematically investigated the mechanical response of single and multimeric ubiquitins to periodic forces. Our work is motivated by the desire to understand protein dynamics under biological repetitive forces as well as by growing theoretical interest in periodically modulated biomolecular systems.[22,28–31] To obtain quantitative insights into dynamic ubiquitin stability, we devised periodic force MD simulations and combined them with a kinetic model. We found a complex, linkage-dependent response that included asymmetric weakening of the protein, shifts in unfolding pathways, and refolding. Our observations are captured using energy landscape models and discussed in light of single-molecule experiments and physiological forces.

Results

Protein unfolding with constant velocity and periodic forces

We combined two approaches, MD simulations and a kinetic model, to probe ubiquitin's nano-mechanical response to periodic forces. To obtain complete pictures of its stability, we probed the protein with a broad range of force frequencies and amplitudes. In our MD simulations, we generated a modulation force by periodic displacement of a spring connected to a residue or a terminus of the protein (see Fig. 1 and Materials and Methods). The effective force experienced by the protein is periodic with a defined force amplitude (see below). The simulations were based on a coarse-grained model that allowed access to sinusoidal forces with frequencies spanning 4 orders of magnitude ($v = 6.3~\mu s^{-1}$, $63~\mu s^{-1}$, $630~\mu s^{-1}$, and $6.3~ns^{-1}$). Since the characteristic mechanical relaxation time of ubiquitin, τ_r, was ≈ 3 ns in our model (see Materials and Methods), $v = 6.3~ns^{-1}$ corresponds to a high-frequency regime, $v = 630~\mu s^{-1}$ to an intermediate-frequency regime, and $v = 6.3$ and $63~\mu s^{-1}$ to a low-frequency regime. As described below, low-frequency forces are of particular biological interest. The integration time step in our simulations is 0.8 ps and, thus, 2 to 3 orders of magnitude shorter than the relaxation time of the protein or the period of the highest frequency force. At each frequency, we investigated five oscillation amplitudes (0.5, 1.0, 1.5, 2.5, and 3.75 nm) that cover the range of amplitudes exerted by biological machines and in mechanical single-molecule experiments.[6,14,18,56–61] We included a sinusoidal driving force in a constant velocity (CV) pulling protocol that is commonly used in forced protein
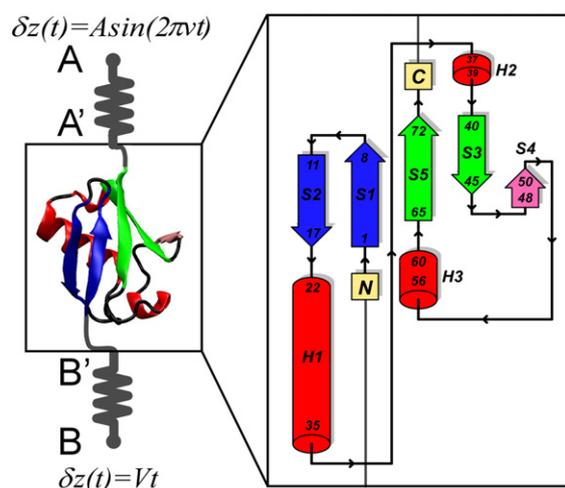
Fig. 1. Unfolding ubiquitin with periodic forces. Two springs flank ubiquitin (Ubq-1) or a ubiquitin trimer (Ubq-3). In periodic force simulations, point A is displaced with constant amplitude (A) and frequency (v), while point B is displaced with CV (V). Inset: topology diagram of ubiquitin showing a mixed α–β-fold with α-helices H1 to H3 and β-strands S1 to S5.
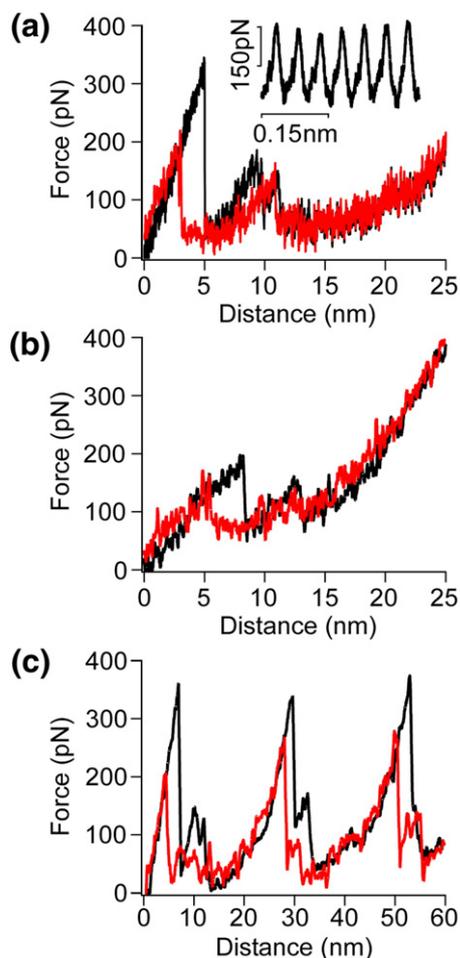
Fig. 2. F–D curves of Ubq-1 and Ubq-3 unfolding. (a) End-to-end unfolding of Ubq-1 without (black trace) and with a periodic force (red trace; $A = 2.5$ nm, $v = 63$ μs^{-1}). Inset: effective force applied to the protein as measured through the periodic extension of spring A–A' (also see Fig. 1). Shown here are the first 0.3 nm of the trace. Periodic force application is observed for the entire traces (also see the main text for details). (b) Unfolding of C-Lys48-linked Ubq-1 with a periodic force ($A = 2.5$ nm, $v = 63$ μs^{-1}). (c) End-to-end unfolding of Ubq-3 without (black trace) and with periodic forces (red trace; $A = 2.5$ nm, $v = 6.3$ μs^{-1}). Curves were averaged over the period of force for visual clarity.

unfolding experiments and simulations (Fig. 1).[33] This implementation has two advantages. Firstly, we can use our results to explain single-molecule experiments of CV protein unfolding with periodic forces. Secondly, we adjusted the number of oscillations per unit length of a translated molecule (V/v) to range from 2.1 nm^{-1} to 2.1 μm^{-1}, in agreement with biological machines such as the Phi29 packaging motor (≈ 0.5 nm^{-1})[6] or the ClpXP proteasome (≈ 2 nm^{-1}).[18,61]

Periodic forces weaken ubiquitin

Our systematic MD investigation begins with a single ubiquitin domain (Ubq-1) tethered at the N-terminus with the periodic force applied to the C-terminus. Figure 2a shows a force–displacement (F–D) curve of Ubq-1 unfolded with CV and a sinusoidal force ($A = 2.5$ nm, $v = 63$ μs^{-1}, red trace) together with a curve for conventional CV unfolding (black trace). F–D traces were averaged over the oscillation period both for visual clarity and for theoretical analysis (see below). The most pronounced effect of the periodic force is the weakening of Ubq-1, that is, reduced peak unfolding forces. For reasons discussed below, we focused our analysis on the main unfolding peak of Ubq-1, which occurs at extensions of ≈ 2–5 nm. A complete frequency- and amplitude-dependent analysis of the decrease in the most probable unfolding force, δF, is shown in Fig. 3. From Fig. 3a, it becomes clear that increased oscillation amplitudes result in decreased unfolding forces. For instance, in the low-frequency regime ($v = 63$ μs^{-1}), unfolding forces are only marginally lowered for $A = 0.5$ nm ($\delta F = 9 \pm 13.4$ pN, averaged over $N = 50$ trajectories), while for $A = 3.75$ nm, the decrease in forces is 159.2 ± 11.6 pN ($\approx 46\%$ of the CV unfolding force of 344.4 ± 3.0 pN, $N = 50$). We also observed that the impact of low-frequency modulations is much stronger than that at higher frequencies. For $v = 6.3$ ns^{-1}, even amplitudes of 3.75 nm do not lower unfolding forces significantly ($\delta F = 0.8 \pm 10.4$ pN, $N = 50$, Fig. 3a). Along these lines, the results indicate the existence of an empirical, frequency-dependent threshold of amplitude below which the periodic forces have no effect. For $v = 6.3$ and 63 μs^{-1}, the threshold is ≈ 1.0 nm, whereas for $v = 630$ μs^{-1}, it shifts to ≈ 2.5 nm. Intuitively, the frequency-dependent modulation of Ubq-1 can be understood by noting that high-frequency forces may be too rapid to be followed by the protein, which effectively feels the constant (DC) component. Similar trends are observed for the second and third unfolding peaks (data not shown). Detailed analysis of these peaks is impeded as Ubq-1 unfolding pathways change in an amplitude- and frequency-dependent manner and because these unfolding intermediates are connected to the periodic force by a nonlinear linker (see below).

Kinetic model for periodic force protein unfolding

To quantitatively understand the dynamic stability of Ubq-1, we solved a kinetic model for protein unfolding with a sinusoidal force. The assumption of a sinusoidal force is not restrictive since any periodic function can be reduced to a sum over sinusoidal components by Fourier analysis. Let us first consider an unbinding or unfolding process under the action of a DC force, F, modulated with a time-dependent (AC) force

$$f = f_0 \sin 2\pi v t \qquad (1)$$

of amplitude f_0 and frequency v. The relevant timescales are the period of the AC force, $T_0 = 1/v$, the relaxation time of the protein, τ_r, and the lifetime of the folded state, τ_F. If τ_r is short in comparison to
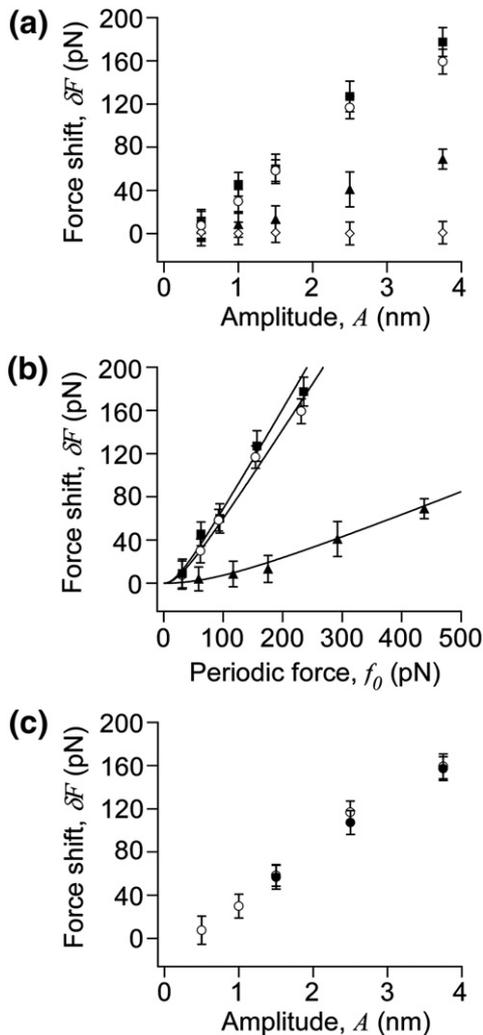
Fig. 3. Periodic forces weaken Ubq-1. (a and b) Decrease in peak unfolding force as a function of purely periodic oscillation amplitudes (a) and force amplitudes (b) for $v = 6.3$ μs^{-1} (squares), $v = 63$ μs^{-1} (circles), $v = 630$ μs^{-1} (triangles), and $v = 6.3$ ns^{-1} (diamonds). It becomes clear that low-frequency forces significantly lower the stability of the protein and thereby catalyze unfolding. High-frequency oscillations result in marginally lowered unfolding forces and large force amplitudes. Continuous lines in (b) are fits with Eq. (5). (c) A virtually identical decrease in peak force is observed for periodic forces [open circles, $v = 63$ μs^{-1}, data taken from (a)] and stochastic, repetitive forces (filled circles, see the text for details). In (a)–(c), each data point is an average of 50 single-molecule traces ±SD.

T_0, that is, $\tau_r/T_0 < 1$, the reaction rate follows the instantaneous potential quasi-statically and is given by[62,63]

$$\kappa = \kappa(F)e^{\beta f_0 \sin 2\pi v t \delta x_t} \tag{2}$$

where $\beta = (k_B T)^{-1}$, δx_t is the location of the transition state along the mechanical reaction coordinate, and $\kappa(F) = \kappa_0 \exp(\beta F \delta x_t)$ is the unfolding rate in the DC case with the natural unfolding rate given by the Kramers formula, $\kappa_0 = 1/\tau_F \sim e^{-\beta \Delta U}$ (ΔU denotes the

height of the energy barrier). As long as T_0 is short in comparison to τ_F, that is, $T_0/\tau_F < 1$, the relevant quantity is not the instantaneous unfolding rate, κ, but rather the effective rate, $\kappa*$, averaged over the period of the force

$$\kappa* = \frac{\kappa(F)}{T_0} \int_0^{T_0} e^{\beta f_0 \sin 2\pi v t \delta x_t} dt = \kappa(F) I_0(f_0/f_\beta) \tag{3}$$

where I_0 is the modified Bessel function of the first kind and $f_\beta = (\delta x_t \beta)^{-1}$ is the characteristic thermal force scale. In the small noise intensity limit considered here, $f_0 > f_\beta$, and using the asymptotic form of the Bessel function for large arguments, $I_0(z) \approx \frac{1}{\sqrt{2\pi z}} e^z + ...$, we obtain $\kappa* = \kappa(F) \frac{1}{\sqrt{2\pi \beta f_0 \delta x_t}} e^{\beta f_0 \delta x_t}$. Thus, the unfolding rate of the protein is enhanced with respect to the non-oscillating case by the factor that depends exponentially on the amplitude of the periodic force.

The problem becomes more complicated for higher frequencies where the quasi-static approximation no longer holds. However, for weak modulation forces, $f_0 \leq \frac{4U}{\delta x_t}$, Eq. (3) may be generalized in the following form

$$\kappa*(F) = \kappa(F) I_0\left(\frac{f_0}{f_\beta} \frac{\eta(v)}{\delta x_t}\right), \tag{4}$$

where $\tilde{\eta}(v) = -\int_{-\infty}^{\infty} \frac{dx^0}{dt} e^{i2\pi vt} dt$ is the so-called logarithmic susceptibility with $x^0(t)$ being an optimal trajectory along the reaction coordinate.[64] This optimal trajectory is a time-reversed trajectory from the transition state to the minimum of the potential well obtained by solving the equations of motion in the absence of both periodic modulation and random noise.[64,65] In the low-frequency limit ($v \to 0$), η approaches δx_t and Eq. (3) is recovered. In the high-frequency regime ($v \to \infty$), η approaches zero and the standard result corresponding to the escape over the unmodulated barrier is recovered.

In unfolding by CV pulling the force on the protein is continuously rising and $\kappa*(F)$ increases with time. The quantity of interest is the most probable unfolding force, $\tilde{F}$, which may be obtained by considerations similar to those of Evans and Ritchie,[63] this time, however, applied to the effective rate of Eq. (4). This leads to $\tilde{F} = \tilde{F}_0 - \delta F$, where $\tilde{F}_0$ is the rupture force in the absence of modulation and

$$\delta F = f_\beta \ln I_0\left(\frac{f_0}{f_\beta} \frac{\eta(v)}{\delta x_t}\right) \tag{5}$$

is the force shift due to the periodic force. In the limit $f_0 > f_\beta$, we obtain $\delta F = \frac{1}{\delta x_t} f_0 \eta(v) - \frac{f_\beta}{2} \ln 2\pi \frac{f_0}{f_\beta} \frac{\eta(v)}{\delta x_t} + ...$ Finally, in the quasi-static limit, $v \to 0$, $\delta F = f_0 - \frac{f_\beta}{2} \ln 2\pi \frac{f_0}{f_\beta} + ...$; thus, in this case, the most probable rupture force is predicted to shift with respect to the unmodulated case on the scale of f_0. Contrastingly, δF vanishes in the high-frequency limit.

Comparison of kinetic model and simulations

We applied Eq. (5) to quantitatively understand the force shifts measured in the simulations. In the
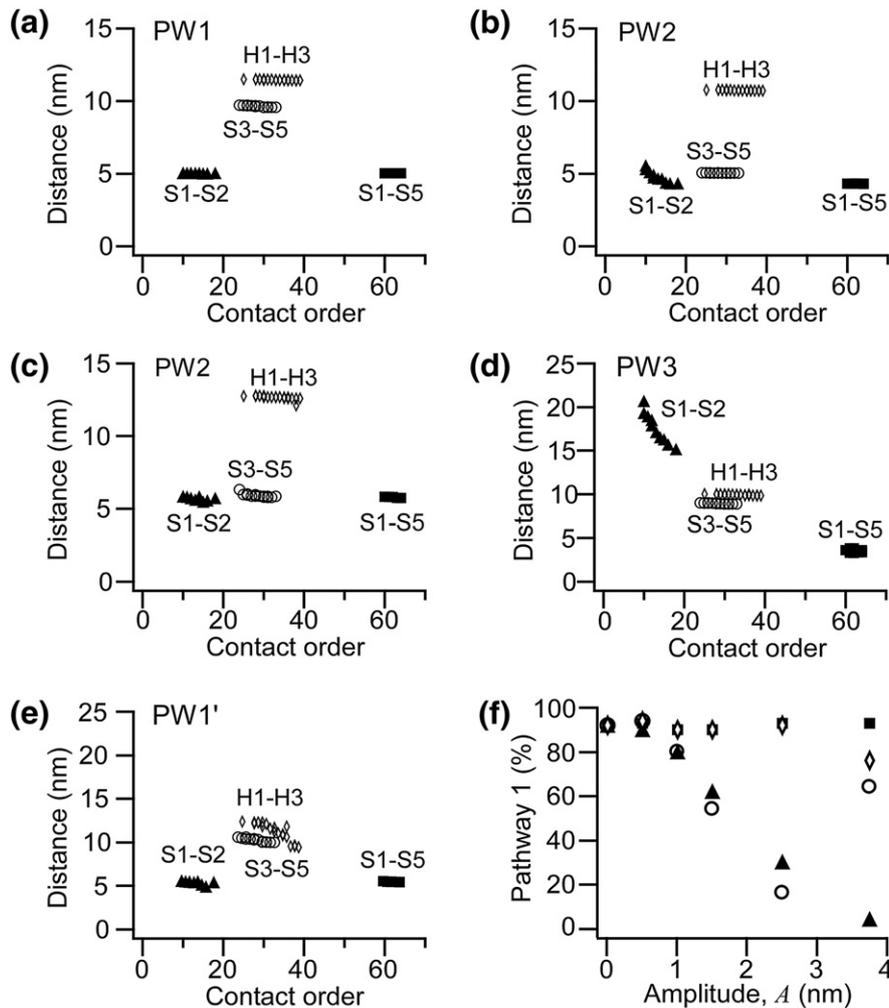
Fig. 4. Scenario diagrams reveal unfolding pathways of Ubq-1. Each symbol indicates the rupture of a native contact at a characteristic distance and contact order. For visual clarity, only contacts between major secondary structures (Fig. 1) excluding contacts between S2 and H1 or those between S3 and S4 are shown in (a) to (e). (a) Pathway (PW) 1 observed when pulling at the C- or N-terminus without periodic force ($V = 3$ nm/μs). (b) Pathway 2 observed in the presence of a C-terminal periodic force ($A = 2.5$ nm, $v = 630$ μs^{-1}, $V = 3$ nm/μs). (c) Pathway 2 measured by pulling at the C-terminus with fast velocity ($V = 30$ nm/μs). (d and e) Unfolding pathway measured by pulling at the N-terminus with a periodic force (d, pathway 3, $A = 2.5$ nm, $v = 63$ μs^{-1}, $V = 3$ nm/μs) or fast velocity (e, pathway 1′, $V = 30$ nm/μs). (f) Population of pathway 1 as a function of oscillation amplitude for $v = 6.3$ μs^{-1} (squares), $v = 63$ μs^{-1} (circles), $v = 630$ μs^{-1} (triangles), and $v = 6.3$ ns^{-1} (diamonds) in the presence of a C-terminal periodic force ($V = 3$ nm/μs).

coarse-grained model, we generated a periodic force (Fig. 2a, inset) by controlling a displacement amplitude (Fig. 1). The force amplitude as defined in Eq. (1) enters Eq. (5) and depends on this displacement amplitude and the frequency-dependent elasticity of the protein. f_0 can be directly obtained by monitoring the extension of the oscillating spring during the simulation (e.g., see Fig. 2a, inset) or in a test simulation at zero pulling speed. Using the latter method, we found that f_0 scales linearly with $k(v) = f_0(v)/A = 61.8$, 63.8, 119.5, and 160.6 pN/nm for $v = 6.3$ μs^{-1}, 63 μs^{-1}, 630 μs^{-1}, and 6.3 ns^{-1}, respectively. Measuring the extension of the spring during the simulation yields equivalent results. Furthermore, the application of a periodic force to the terminus of the protein without the help of a spring produces force shifts that are virtually

identical with those reported here (data not shown). Equation (5) requires an estimate of the thermal force scale, f_β, but not of the height of the energy barrier or natural unfolding rate. The thermal force scale can be obtained by analyzing the pulling speed dependence of the rupture force according to[63]

$$\tilde{F}_0 = f_\beta \ln\left(\frac{kV}{\kappa_0 f_\beta}\right) \qquad (6)$$

where k is the total elastic compliance of the protein-linker system in the quasi-static case. Coarse-grained simulations reported $f_\beta = 16.8$ pN[45] in agreement with experiments.[39,43,66] The only unknown parameter, the logarithmic susceptibility, is determined by fitting force shifts with Eq. (5). For $v = 6.3$ μs^{-1}, 63 μs^{-1}, 630 μs^{-1}, and 6.3 ns^{-1}, we find
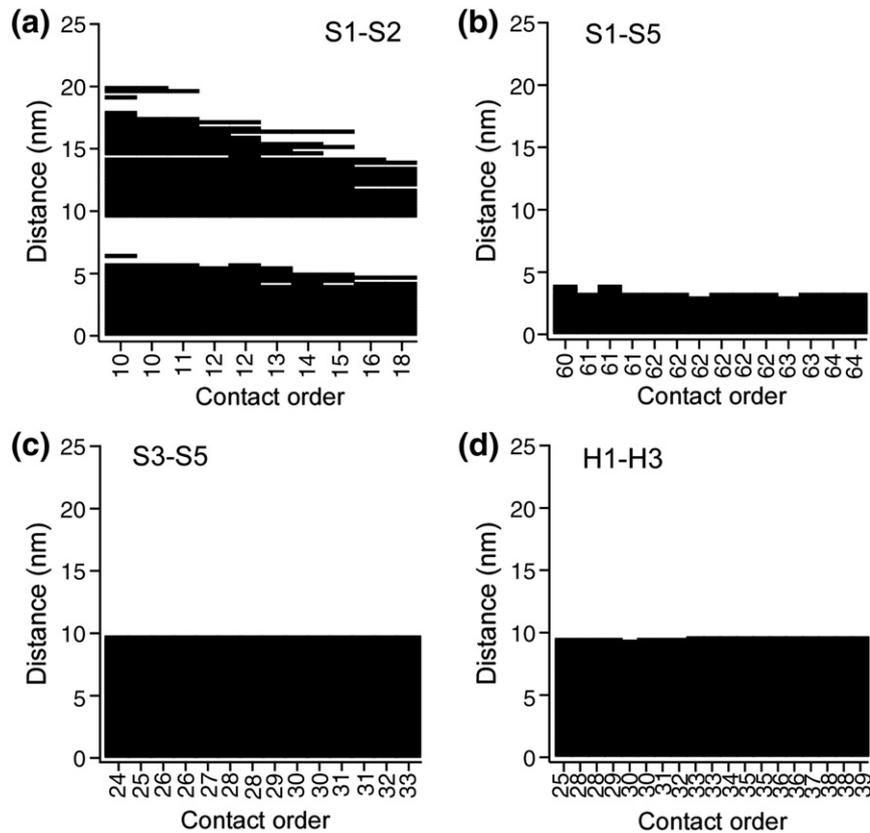
Fig. 5. Refolding of Ubq-1 unfolded with an N-terminal periodic force. Contacts in four groups of secondary structures are shown. Black regions indicate the presence of a contact at a particular distance. Transient refolding is observed for contacts between β-strands S1 and S2 after the initial rupture at ≈5 nm extension (a). In contrast, contacts between other secondary-structure elements (β-strands S1 and S5, β-strands S3 and S5, and α-helices H1 and H3) do not show refolding (b to d).

$\eta(v)/\delta x_t = 0.98$, 0.88, 0.23, and 0.02, respectively. Hence, as predicted above, $\eta(v)$ approaches δx_t in the quasi-static regime and zero in the high-frequency case. The excellent agreement between MD simulations and the kinetic model (Fig. 3b) indicates that unfolding forces are lowered at low oscillation frequencies due to a quasi-static increase in transition rate over the energy barrier. In the high-frequency case, the protein is not susceptible to the periodic force and effectively responds to the DC component.

Periodic forces shift unfolding pathways

We also noticed shifts in the unfolding pathways of Ubq-1. In CV simulations, three force peaks are observed (Fig. 2a, black trace), each of which corresponds to a group of secondary structures. We analyzed these unfolding events using scenario diagrams (Fig. 4), where the last distance at which a native contact persisted is plotted against contact order (the primary sequence distance of the residues forming this contact). The scenario diagram shows that the main force peak at ≈2 to 5 nm extension is associated with separating two pairs of parallel β-strands, S1–S5 and S1–S2. It was previously shown that S1–S5 contacts act as a mechanical clamp

responsible for the protein's high mechanical resistance.[48,67] In a subsequent event, β-strands S3 and S5 are separated well after the other β-strands unfolded (also see Fig. 7, top, for structures of unfolding intermediates). In this unfolding pathway (termed pathway 1, Fig. 4a), the unfolding sequence reads 'S1–S5, S1–S2, S3–S5, H1–H3' in agreement with existing experimental[39,41–44] and computational studies.[45–52] At these pulling speeds ($V = 3$ nm/μs), pathway 1 holds irrespective if the protein was pulled at the C- or at the N-terminus.

Contrastingly, in the presence of a periodic force, we frequently noticed a second class of traces with only two peaks (Fig. 2a, red trace). Analysis using a scenario diagram showed that these traces originate from a unique unfolding sequence (pathway 2, Fig. 4b). Here, β-strands S3 and S5 break cooperatively with the first event. Interestingly, this pathway is not populated at $v = 6.3$ μs^{-1}, again indicating that protein unfolding is quasi-static at the lowest frequency. For all other frequencies, increasing amplitudes result in increased population of pathway 2 (Fig. 4f). Pathway shifts may originate from a reduction of the energy barrier associated with β-strands S3 and S5, potentially by rapid and large transient components of the periodic force (Fig. 3b). To test this hypothesis, we compared pathway 2 to
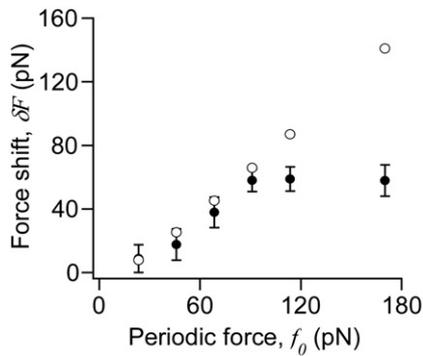
Fig. 6. Stability of C-Lys48-linked Ubq-1. Force shifts measured in simulations (filled circles) are predicted by the kinetic model (open circles). To predict force shifts, Eq. (5) was applied as described in the text.

pathways obtained at faster pulling velocity ($V = 30$ nm/μs) but without periodic forces (Fig. 4c). Indeed, pathway 2 was observed in 74% of the traces ($N = 30$) and the remaining traces showed a pathway similar to pathway 1 (pathway 1′). Pathway 1′ is also detected when Ubq-1 is unfolded from the N-terminus with high pulling velocities (see below).

Repetitive forces with broadly distributed frequencies

Biological machines operate in stochastic working cycles, and their effective force frequencies are random. In particular, it was shown that dwell times between ATP-powered steps of cytoskeleton-associated motor proteins are broadly distributed.[68,69] For these reasons, we extended our MD simulations to repetitive forces with variable periods. The periods were a random quantity with an exponential probability distribution $P(t) = \tau_m^{-1} \exp\left(-\frac{t}{\tau_m}\right)$. We tuned the average of this distribution, τ_m, to the previously analyzed period of $\approx 1/63$ μs and examined three oscillation amplitudes (1.5, 2.5, and 3.75 nm). Remarkably, a very similar reduction in unfolding forces of Ubq-1 is observed when these random frequency forces are compared to fixed-frequency forces with the same average period (Fig. 3c). Furthermore, at all amplitudes, we observed a large fraction of traces in which the protein followed unfolding pathway 2 (16%, 80%, and 52% of traces for $A = 1.5$, 2.5, and 3.75 nm; $N = 50$).

Periodic forces at the N-terminus of ubiquitin

We also applied periodic forces to the N-terminus of Ubq-1 for an intermediate amplitude and two frequencies ($A = 2.5$ nm with $\nu = 6.3$ μs^{-1} and 63 μs^{-1}). At $\nu = 63$ μs^{-1}, scenario diagrams revealed a novel unfolding pathway (pathway 3) in 77% of the traces (in the remaining traces, we observed pathway 2, $N = 30$). In pathway 3, the final rupture of β-strands S1 and S2 occurs at the very end of the

unfolding process (Fig. 4d, triangles). The late unfolding of this most N-terminal region of Ubq-1 is counterintuitive and not observed for rapid pulling at the N-terminus: At $V = 30$ nm/μs, S1–S2 contacts always break at extensions of ≈ 5 nm (pathway 1′, $N = 30$, Fig. 4e, triangles). For these reasons, and as scenario diagrams only highlight the last time point at which a contact still persisted, we inspected the evolution of S1–S2 contacts more closely. This analysis revealed that S1–S2 contacts always break very early but can reform in the presence of the periodic force (Fig. 5a). Refolding of the S1–S2 structure was observed in all traces at $\nu = 6.3$ μs^{-1} and 63 μs^{-1}, and the intermediate has a remarkable stability persisting until the protein is extended to ≈ 15 nm. Refolding was not detected for other secondary-structure elements (Fig. 5b–d).

A subtle but significant difference between pathway 2 (recorded when pulling at the C-terminus) and pathways 1′ and 3 (recorded when pulling at the N-terminus) points towards additional pathway shifts induced by transient forces. In the latter case, α-helices H1 and H3 and β-strands S3 and S5 rupture simultaneously (Fig. 4d and e, diamonds and circles).

Linkage-dependent stability of ubiquitin

Covalent attachment of multimeric ubiquitins tethered between their C-terminus (C) and lysine residue 48 (Lys48) targets proteins to degradation pathways.[38] A potential role of ubiquitin's mechanical stability during proteasomal substrate unfolding[25,39,40] led us to investigate C-Lys48-linked Ubq-1 with periodic forces at the C-terminus (Fig. 2b). In the absence of the periodic force, we measured unfolding forces of 196.1 ± 3.5 pN ($N = 25$), in agreement with experiments reporting smaller stability of this linkage compared to end-to-end unfolding.[39] For $\nu = 6.3$ μs^{-1} and $A = 0.5$, 1.0, 1.5, and 2.0 nm, we observed peak unfolding forces of 187.8 ± 8.8, 178.9 ± 9.8, 158.5 ± 9.6, and 138.4 ± 7.0 pN, respectively ($N = 25$ for each amplitude). We applied Eq. (5) to predict the force shifts of C-Lys48-linked Ubq-1 with $f_0/A = 45.3$ pN/nm, $f_\beta = 12.55$ pN [from Eq. (6), data not shown] and a $\eta(\nu)/\delta x_t$ close to 1 [$\eta(\nu)/\delta x_t = 0.9$]. For these relatively small amplitudes, the force shifts predicted by Eq. (5) are close to those determined in the simulation (Fig. 6). However, for larger amplitudes, force shifts saturated with $\tilde{F} = 137.6 \pm 7.7$ and 138.5 ± 9.8 pN for $A = 2.5$ and 3.75 nm and diverged from the theoretical prediction (Fig. 6). This can be understood by noting that Eq. (4) was obtained in the linear response approximation, that is, assuming that the energy associated with the periodic force [$\sim f_0 \eta(\nu)$] is small compared to the barrier height.[64] However, the barrier height is constantly lowered during stretching and thus corrections to Eq. (4) may become important. These corrections decrease the transition rate[70] and the shift in rupture force should become smaller at large amplitudes as observed here. Finally, we note that C-Lys48-linked Ubq-1 is less susceptible to the

periodic force than Ubq-1 unfolded from its ends (e.g., $\delta F \approx 58$ pN for C-48 linkage and 182 pN for end-to-end unfolding at $A = 3.75$ nm).

Unfolding a multi-domain protein

We also examined a multi-domain protein composed of three ubiquitin domains (Ubq-3). Fig. 2c compares CV unfolding of Ubq-3 with and without periodic forces applied to the C-terminus. A similar behavior as for Ubq-1 is observed. At $A = 2.5$ nm and $v = 6.3$ μs^{-1} (63 μs^{-1}), peak forces are significantly lowered by 131 ± 12 (119 ± 6), 84 ± 10 (25 ± 10), and 80 ± 8 (10 ± 8) pN for the domain that unfolds first, second, and third, respectively ($N = 12$ for each frequency and domain). While the force shifts of the domain that unfolded first are considerable, one observes smaller and similar force shifts for the other domains. There also are significant pathway shifts for $v = 63$ μs^{-1} but not for $v = 6.3$ μs^{-1}. At $v = 63$ μs^{-1}, pathway 2 is populated with 92% and 75% for the domain that unfolded first and second, respectively ($N = 12$). In CV simulations with and without periodic forces, we were unable to reliably detect unfolding pathways in the domain that unfolded last.

Discussion

Theoretical approaches to biological repetitive forces

Proteins experience repetitive forces in many physiological contexts.[6,16–23] For instance, it is vital for cellular protein unfolding machineries to periodically release substrates, allowing them to adjust their conformation and prevent entanglements.[21,40] Similarly, instrumentation has been developed to probe single-molecule protein mechanics with periodic forces.[56–60] We set out to theoretically probe the effects of periodic forces on the stability of ubiquitin. Similarly to a biological machine, we generated a repetitive pulling force through periodic displacement of the protein in coarse-grained MD simulations.[71,72] Coarse-grained representations are widely used to study protein (un)folding,[73,74] and Gō-like models have been shown to accurately reproduce experiments and atomistic models of mechanical protein denaturation.[52,75] Using coarse-grained simulations, we were able to access microsecond timescales in a statistically significant number of single-molecule trajectories. Simulation times of individual trajectories range from 0.83 to 20.0 μs (depending on pulling velocity and number of domains) and are necessary to model forces with periods orders of magnitude longer than the relaxation time of ubiquitin. Such low-frequency forces are of particular physiological relevance since biological machines are likely unable to generate forces faster than their own relaxation times, and concerted conformational changes in proteins typically occur on micro- or millisecond timescales. We

also adjusted the oscillation amplitudes and the number of oscillations per unit protein length to be close to those of biological machines (see Results). Finally, biological machines can operate against maximal forces on similar scales as those reported here (≈ 1–100 pN)[76–80] and the periodic forces generated in our model thus may mimic those encountered by proteins in native contexts.

Repetitive forces catalyze protein unfolding

To complement MD simulations, we solved a kinetic model that traces the effect of a repetitive force on protein stability without precise knowledge of the height of the energy barrier that confines the folded state. The decreased peak forces in MD simulations are well described in the complete range of frequencies and amplitudes (Fig. 3b). Ubq-1 is unable to respond to high-frequency periodic forces ($v \geq 630$ μs^{-1}). At lower frequencies ($v \leq 63$ μs^{-1}), the force required to overcome ubiquitin's first energy barrier is significantly decreased even at moderate amplitudes (Figs. 2a and 3b). In simulations with exponentially distributed force periods, we found a virtually identical reduction in unfolding forces as for fixed frequencies. We interpret this result by noting that the mean frequency of the stochastic force lies in the quasi-static regime (see next paragraph) and forces with frequencies ≤ 63 μs^{-1} weaken the protein by a similar amount (e.g., see Fig. 3). Consequently, one would only expect a small (or no) change in peak force when the two types of simulations are compared. However, note that the presence of high-frequency forces manifests itself in the stochastic simulations in terms of shifts in unfolding pathways. The effective force pattern generated by this particular protocol may approximate low-frequency enzymatic cycles (also see below). Furthermore, through Fourier analysis, one should be able to reduce any time-dependent force to a sum over trigonometric components. These results prompt us to propose that repetitive forces generated by biological machines may significantly weaken proteins and 'catalyze' their unfolding. In the case of Ubq-1, agreement of simulations and kinetic model further suggests that there is no shift in the position of the first energy barrier or complex changes in this part of the protein's energy landscape (however, see below).

Predicting dynamic protein stability on biological scales

We propose that these two theoretical models provide a framework for understanding protein mechanics in response to complex, repetitive forces. Firstly comparing force frequency and protein relaxation time allows estimating changes in dynamic protein stability. For Ubq-1, the period of the force needs to be at least 5-fold lower than the relaxation time to exert a measurable effect on unfolding forces and pathways. Secondly, the kinetic model quantitatively predicts the weakened
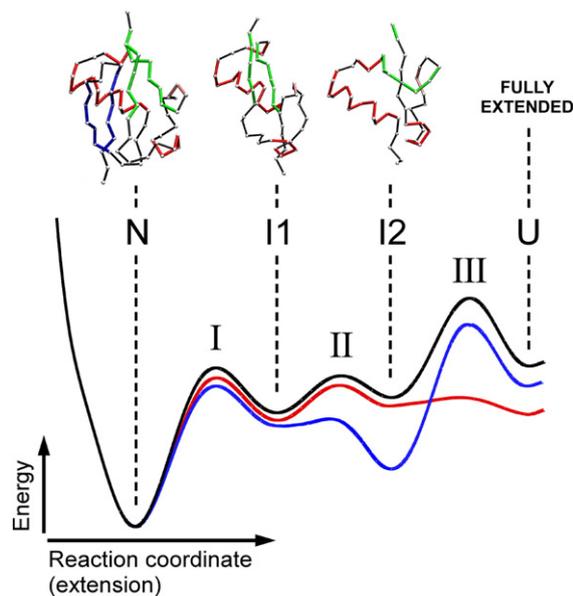
Fig. 7. Snapshots of unfolding intermediates (top) and energy landscape for mechanical ubiquitin unfolding (bottom). Two unfolding intermediates (I1 and I2) separate the native state (N) from the unfolded state (U) on the energy surface. β-Strands S1 and S2 are shown in blue, S3 and S5 in green, and S4 in magenta and α-helices H1 to H3 are shown in red (also see Fig. 1). Energy barrier I corresponds to contacts of two pairs of β-strands (S1 and S5, S1 and S2) while energy barriers II and III represent contacts of β-strands S3 and S5 and α-helices H1 and H3, respectively (Fig. 4a). I1 is not observed in the presence of a C-terminal periodic force (Fig. 4b). We propose that barrier II is not rate limiting and the protein unfolds downhill to I2 (blue line). In apparent contrast, I2 is not observed with an N-terminal periodic force (Fig. 4e) and the protein unfolds directly to U (red line).

mechanics of the protein, particularly in the biologically relevant low-frequency limit (e.g., see Fig. 6). Following Eq. (5), the decrease in protein stability solely depends on the amplitude of oscillating force (f_0) and thermal force scale, which includes transition state position and temperature ($f_\beta = k_B T / \delta x_t$). An increased separation of transition state and folded state on the reaction coordinate results in lowered unfolding forces.

One should note that even the lowest frequency tested in our simulations is several orders of magnitude higher than those of forces generated by biological machines. However, kinetic modeling suggests that we successfully sampled a low-frequency regime that likely extends to much slower processes. Since $\eta(\nu)$ approaches δx_t for the lowest frequencies, we already recover the quasi-static transition rate of Eq. (3) in that regime, with vanishing frequency-dependent terms. Accordingly, only a very small additional weakening is observed when the frequency is lowered from $\nu = 63$ to $6.3 \ \mu s^{-1}$ as the ratio of force frequency and protein relaxation time is important. Our results thus suggest that even lower force frequencies very likely elicit quantitatively similar responses such as those described here for the lowest frequencies. Finally, our simulations may reflect current limitations in computing speed even for simplified molecular models.

Shifts in unfolding pathways on a simple energy surface

At slow pulling speeds or with slow periodic forces, Ubq-1 unfolds in the well-known sequence of β-strands S1 and S5, S1 and S2, and S3 and S5 and of α-helices H1 and H3 (pathway 1, Fig. 4a) irrespective at which terminus the force was applied (see Fig. 7, top, for structures of unfolding intermediates). However, periodic forces with $\nu \geq 63 \ \mu s^{-1}$ revealed new dominant unfolding pathways (pathways 2 and 3, Fig. 4b and d). These pathways are similar to the ones observed when the protein with higher pulling speeds is unfolded, and thus, one could speculate that transient forces trigger pathways shifts. The pathway shifts can be qualitatively explained on a one-dimensional energy surface. In this simple model (Fig. 7, black trace), the native state and two unfolding intermediates are each confined by an energy barrier. In pathway 2 recorded with C-terminal periodic forces, our data show that unfolding intermediate 1 (I1) is not populated; that is, S3–S5 contacts break simultaneously with S1–S5 and S1–S2 contacts. This suggests that a second, rate-limiting energy barrier does not exist (Fig. 7, blue trace) and that the protein unfolds 'downhill' to I2 after crossing the first energy barrier. This model is also supported by the above kinetic analysis of the first unfolding peak. A one-barrier model describes the force shift of this peak for all amplitudes and frequencies (i.e., irrespective of the unfolding pathway), and thus, S3–S5 contacts likely never contribute to this energy barrier. The application of a periodic force to the N-terminus of Ubq-1 induced a similar response: α-helices H1 and H3 unfold early and the third energy barrier may be lowered in this case (Fig. 7, red trace).

Refolding of the N-terminal region of ubiquitin and the role of local interactions

The dynamic response of Ubq-1 is not limited to shifts in unfolding pathways. A periodic force applied to the N-terminus triggered transient refolding of β-strands S1 and S2 to a stable (un-)folding intermediate different from the molten globule-like state reported before.[42,46,81,82] Furthermore, marked difference between unfolding pathways observed with N-terminal or C-terminal perturbations allows us to propose that Ubq-1's response to periodic forces is asymmetric. In the case of C-terminal perturbations, β-strands located close to the C-terminus are under large local stress resulting in modulation of their energy barrier. For N-terminal forces, β-strands located close to this terminus are unfolded and refolded and the energy

barrier of H1–H3 contacts is lowered. In these examples, periodic forces with $v \geq 63$ μs^{-1} effectively probe 'local' interactions, while stretch–compression cycles are uniform and pathway shifts are not detected at slower oscillations. It is interesting to note that local interactions determine protein stability *in vivo*, for example, during protein unfolding at the proteasome or protein import into mitchondria.[3]

Repetitive forces modulate energy landscape paths

Energy landscapes of proteins are well known to dynamically adapt to cues such as point mutations, ligand binding, solvent, or temperature by changing the position, height, and roughness of local energy features.[83–86] Our results extend these views by demonstrating that a periodic force can change unfolding pathways in a small protein. In the case of ubiquitin, these pathway shifts are explained by a nontrivial change in the effective energy landscape sampled by the protein. This altered choice of paths on the multidimensional energy surface may have implications on how we currently model mechanical processes that occur *in vivo*. It is tempting to use energy landscape paths determined in pulling experiments and simulations as predictors for cellular mechanical responses. However, biological forces may have complex patterns that differ markedly from typical experiments and simulations. Ubiquitin's nontrivial response to a periodic force suggests that effective energy landscape topographies may not be *per se* transferable between mechanical scenarios. Additionally, it was recently shown that repeated release of an electric force accelerated the protein unfolding in a pore through the escape from trapped states and sampling of fast pathways.[21] In the light of these two findings, it appears advantageous to develop energy landscape models under native-like mechanical conditions.

C-Lys48-linked ubiquitins are remarkably insensitive to repetitive forces

Ubiquitin chains with domains linked between the C-terminus and Lys48 target proteins to proteasomal degradation pathways. The ubiquitin chain is recognized by the proteasome lid and remains bound to it during substrate unfolding[40] regulated by complex (de-)ubiquitination steps.[87] Different models for ubiquitin's role beyond initial recognition events exist. In one model, it has been proposed that substrate unfolding occurs by pulling against the fold of an anchored ubiquitin.[39,40] In this case, one would expect that ubiquitin's mechanical stability and ubiquitin–proteasome contacts must withstand forces generated by the proteasome.[39,40] Interestingly, single-molecule experiments measured 2- to 3-fold smaller peak forces for C-Lys48-linked ubiquitin when compared to end-to-end unfolding.[39] This finding is somewhat counterintuitive given the potential mechanical function of

C-Lys48-linked monomers. To address this question, we probed Ubq-1 when C-Lys48-linked and when unfolded from its ends. Surprisingly, C-Lys48-linked Ubq-1 responds with a small, maximal reduction of unfolding forces even to large force amplitudes ($\delta F_{max} \approx 58$ pN). Furthermore, similar peak unfolding forces are measured for these linkages at the largest amplitude (138.5 pN for C-Lys48 and 167.0 pN for end to end, $A = 3.75$ nm, Figs. 3 and 6). In case of C-Lys48-linked Ubq-1, contacts between β-strands 3 and 5 are responsible for the protein's mechanical resistance[45,50] without evidence for intermediates that may act as a flexible linker (see case of multi-domain protein below). Our results are thus in line with unique biomechanics of C-Lys48-linked ubiquitin in a simplified model that lacks the proteasome.

Repetitive forces and mechanical fingerprints of multi-domain proteins

Mechanical responses of multi-domain proteins are more than serial combinations of single domains[88,89] with physiologically important signatures.[35,90,91] We took advantage of polyubiquitin to understand how linker elasticity influences the propagation of a periodic force in a biological system. The peak unfolding force of the domain that unfolded first was reduced the most. This can be explained by the fact that each denatured domain acts as a flexible, nonlinear linker. Displacement induces larger periodic forces in a shorter (stiffer) chain than in a longer (softer) chain and effects of periodic modulations become weaker with each unfolded domain. Flexible linkers thus have dynamic mechanical properties in addition to well-studied effects on forced unfolding kinetics.[92,93] Long unstructured domains, such as those of force-bearing proteins,[35,90] may 'filter' periodic forces unless stretched to extreme lengths. We note that the effective mechanical fingerprint of a multi-domain protein is modified by periodic perturbations. Hierarchical unfolding of domains at gradually increasing forces is observed in contrast to CV experiments[93] and CV simulations. Hierarchical unfolding patterns also govern the elasticity of some native multi-domain proteins.[88]

Understanding periodic-force, single-molecule experiments

In the past decade, mechanical, single-molecule experiments revealed force-induced unfolding pathways and kinetics of soluble and membrane proteins.[36,94,95] Atomic force microscopy techniques were developed to probe the complex mechanics and viscoelastics of single proteins.[56–60] In these experiments, the atomic force microscopy cantilever is sinusoidally oscillated, resulting in a periodic force applied to the sample. Such experiments have not been conducted on ubiquitin, but we were nevertheless able to explain experiments with other proteins with the above principles. Higgins *et al.*

reported lowered peak forces during the periodic force unfolding of an immunoglobulin 91 octamer at a frequency lower than the protein relaxation time.[57] The peak unfolding forces were independent of the number of unfolded domains, which can be explained by considering that all analyzed domains were connected to the force probe *via* a flexible linker. The experiments of Higgins *et al.* and others also showed that periodic forces change unfolding pathways of carbonic anhydrase B, immunoglobulins, or the membrane protein bacteriorhodopsin.[56–60] In agreement with our observations on Ubq-3, pathway shifts were observed for all domains of multimeric proteins even if unfolding forces were unaltered.[56,59] In summary, our models explain experimental unfolding forces and pathway shifts. Since these effects can be observed for proteins with different structures and functions, they appear to be the fundamental types of responses to periodic mechanical information.

Conclusions

Little knowledge on the response of proteins to repetitive mechanical perturbations exists, particularly on biologically relevant scales. Here, a periodic force triggered a complex response in the small protein ubiquitin that was dependent on force amplitude and frequency. We found that simple repetitive force patterns are capable of weakening the protein, changing its unfolding pathways, and catalyzing transient refolding of single secondary structures. Many biological forces may have repetitive signatures. We therefore consider a framework for biomechanics in response to periodic forces a starting point to understand (i) mechanisms by which proteins and cells process biological mechanical information and (ii) protein folding and stability *in vivo*.

Materials and Methods

Coarse-grained model

For our geometry-based coarse-grained model, we followed the Gõ-like[71,72] implementation of Cieplak *et al.*[96] The human ubiquitin starting structure (Protein Data Bank ID: 1ubq) was represented by a chain of C^{α} atoms tethered along the backbone by harmonic potentials with minima at 3.8 Å. Effective interactions between residues are split into native and nonnative interactions by checking for overlaps between the enlarged van der Waals surfaces of the residues.[97] Amino acids (*i* and *j*) that overlap are endowed with the effective Lennard–Jones potential $V_{ij} = 4\varepsilon \left[\left(\frac{\sigma_{ij}}{r_{ij}} \right)^{12} - \left(\frac{\sigma_{ij}}{r_{ij}} \right)^{6} \right]$ with energy scale ε and pair-by-pair distances r_{ij}. The length parameters, σ_{ij}, are chosen such that the potential minima correspond pair by pair to the native state distance between the residues. Nonnative contacts are represented by hardcore repulsion to prevent entanglements. Correct chirality is imposed by the angle-dependent term in the Hamiltonian. The over-

damped motion of amino acids in solvent was mimicked using a standard Brownian dynamics algorithm.[98] The integration time step in our simulations is 0.8 ps and thus 2 to 3 orders of magnitude shorter than the relaxation time of the protein or the period of the highest frequency force. This coarse-grained model was recently validated by comparing experimental unfolding forces to those obtained in simulations.[75] The effective, uniform energy parameter ε obeys $kT = 0.3\varepsilon$ for ubiquitin and thus $\varepsilon = 1000$ K $\approx$ 13.8 pN/nm.[45,75] The unfolding forces reported here were scaled with this conversion factor and are in good agreement with experimental ubiquitin unfolding forces for both pulling geometries at the same pulling speeds.[39] We point out that the key results of our work, for example, the agreement of kinetic model and simulations, are not affected by choice of conversion factor that rescales all data uniformly.

The protein was attached to harmonic springs with spring constant $k = 160$ pN/nm yielding a total linkage stiffness of 80 pN/nm (Fig. 1). This stiffness is on the same scale as the stiffness of Ubq-1 in our model (see Results) and corresponds to the upper end of stiffness encountered by proteins *in vivo*[88] and in single-molecule pulling experiments. The effects of more compliant linkers are studied through multi-domain proteins (see Discussion). In CV unfolding without periodic forces, the spring connecting A and A′ is fixed and the spring connecting B and B′ is pulled with CV ($V = 3$ or 30 nm/μs) along the initial end-to-end position vector ($\delta z = Vt$, Fig. 1). In periodic force simulations, point A is displaced in z direction with amplitude A, which determines the force amplitude f_0, and frequency ν ($\delta z = A \sin 2\pi \nu t$), while the second spring moves as described above.

Estimating protein relaxation times

We estimated the relaxation time of the protein to equilibrium, τ_r, in a test simulation. The protein was perturbed by a small external force (≈ 40 pN) that stretched the bonds in the molecule but was too weak to disrupt native contacts. By monitoring the end-to-end length and radius of gyration, we measured the time required to reach a new steady state and this time served as our order of magnitude estimate of τ_r. For Ubq-1, $\tau_r \approx 3$ ns, and for Ubq-3, $\tau_r \approx 27$ ns.

Acknowledgements

References

1. Huang, S., Ratliff, K. S., Schwartz, M. P., Spenner, J. M. & Matouschek, A. (1999). Mitochondria unfold precursor proteins by unraveling them from their N-termini. *Nat. Struct. Biol.* **6**, 1132–1138.

2. Klimov, D., Newfield, D. & Thirumalai, D. (2002). Simulations of beta-hairpin folding confined to spherical pores using distributed computing. *Proc. Natl Acad. Sci. USA*, **99**, 8019–8024.

3. Prakash, S. & Matouschek, A. (2004). Protein unfolding in the cell. *Trends Biochem. Sci.* **29**, 593–600.

4. Shtilerman, M., Lorimer, G. H. & Englander, S. W. (1999). Chaperonin function: folding by forced unfolding. *Science*, **284**, 822–825.

5. Cook, P. (1999). The organization of replication and transcription. *Science*, **284**, 1790–1795.

6. Guo, P. & Lee, T. (2007). Viral nanomotors for packaging of dsDNA and dsRNA. *Mol. Microbiol.* **64**, 886–903.

7. Neuwald, A. F., Aravind, L., Spouge, J. L. & Koonin, E.V. (1999). AAA+: a class of chaperone-like ATPases associated with the assembly, operation, and disassembly of protein complexes. *Genome Res.* **9**, 27–43.

8. Erzberger, J. & Berger, J. (2006). Evolutionary relationships and structural mechanisms of AAA+ proteins. *Annu. Rev. Biophys. Biomol. Struct.* **35**, 93–114.

9. Graumann, P. (2007). Cytoskeletal elements in bacteria. *Annu. Rev. Microbiol.* **61**, 589–618.

10. Hartman, J. J. & Vale, R. D. (1999). Microtubule disassembly by ATP-dependent oligomerization of the AAA enzyme katanin. *Science*, **286**, 782–785.

11. McCarthy, E. & Goldstein, B. (2006). Asymmetric spindle positioning. *Curr. Opin. Cell Biol.* **18**, 79–85.

12. Ingber, D. E. (2006). Cellular mechanotransduction: putting all the pieces together again. *FASEB J.* **20**, 811–827.

13. Vogel, V. & Sheetz, M. (2006). Local force and geometry sensing regulate cell functions. *Nat. Rev. Mol. Cell Biol.* **7**, 265–275.

14. Vale, R. D. (2000). AAA proteins. Lords of the ring. *J. Cell Biol.* **150**, F13–19.

15. Tomkiewicz, D., Nouwen, N. & Driessen, A. (2007). Pushing, pulling and trapping-modes of motor protein supported protein translocation. *FEBS Lett.* **581**, 2820–2828.

16. De Los Rios, P., Ben-Zvi, A., Slutsky, O., Azem, A. & Goloubinoff, P. (2006). Hsp70 chaperones accelerate protein translocation and the unfolding of stable protein aggregates by entropic pulling. *Proc. Natl Acad. Sci. USA*, **103**, 6166–6171.

17. Gaume, B., Klaus, C., Ungermann, C., Guiard, B., Neupert, W. & Brunner, M. (1998). Unfolding of preproteins upon import into mitochondria. *EMBO J.* **17**, 6497–6507.

18. Kenniston, J., Baker, T., Fernandez, J. & Sauer, R. (2003). Linkage between ATP consumption and mechanical unfolding during the protein processing reactions of an AAA+ degradation machine. *Cell*, **114**, 511–520.

19. Mokranjac, D. & Neupert, W. (2005). Protein import into mitochondria. *Biochem. Soc. Trans.* **33**, 1019–1023.

20. Shingyoji, C., Higuchi, H., Yoshimura, M., Katayama, E. & Yanagida, T. (1998). Dynein arms are oscillating force generators. *Nature*, **393**, 711–714.

21. Tian, P. & Andricioaei, I. (2005). Repetitive pulling catalyzes co-translocational unfolding of barnase during import through a mitochondrial pore. *J. Mol. Biol.* **350**, 1017–1034.

22. Zaikin, A. & Poschel, T. (2005). Peptide-size-dependent active transport in the proteasome. *Europhys. Lett.* **69**, 725–731.

23. Zhang, J., Li, W., Sanders, M., Sumpio, B., Panja, A. & Basson, M. (2003). Regulation of the intestinal epithelial response to cyclic strain by extracellular matrix proteins. *FASEB J.* **17**, 926–928.

24. Hochstrasser, M. & Wang, J. (2001). Unraveling the means to the end in ATP-dependent proteases. *Nat. Struct. Biol.* **8**, 294–296.

25. Lee, C., Schwartz, M. P., Prakash, S., Iwakura, M. & Matouschek, A. (2001). ATP-dependent proteases degrade their substrates by processively unraveling them from the degradation signal. *Mol. Cell*, **7**, 627–637.

26. Navon, A. & Goldberg, A. L. (2001). Proteins are unfolded on the surface of the ATPase ring before transport into the proteasome. *Mol. Cell*, **8**, 1339–1349.

27. Vidybida, A. (1987). Modification of the potential function of a mechanical system caused by periodic action. *Acta Mech.* **67**, 183–190.

28. Braun, O., Hanke, A. & Seifert, U. (2004). Probing molecular free energy landscapes by periodic loading. *Phys. Rev. Lett.* **93**, 158105.

29. Lin, H., Sheng, Y., Chen, H. & Tsao, H. (2008). Forced dissociation of a biomolecular complex under periodic and correlated random forcing. *J. Chem. Phys.* **128**, 084708.

30. Lomholt, M., Urbakh, M., Metzler, R. & Klafter, J. (2007). Manipulating single enzymes by an external harmonic force. *Phys. Rev. Lett.* **98**, 168302.

31. Pereverzev, Y. & Prezhdo, O. (2006). Dissociation of biological catch-bond by periodic perturbation. *Biophys. J.* **91**, L19–L21.

32. Leckband, D. & Israelachvili, J. (2001). Intermolecular forces in biology. *Q. Rev. Biophys.* **34**, 105–267.

33. Sotomayor, M. & Schulten, K. (2007). Single-molecule experiments in vitro and in silico. *Science*, **316**, 1144–1148.

34. Bustamante, C., Chemla, Y., Forde, N. & Izhaky, D. (2004). Mechanical processes in biochemistry. *Annu. Rev. Biochem.* **73**, 705–748.

35. Linke, W. & Grutzner, A. (2008). Pulling single molecules of titin by AFM—recent advances and physiological implications. *Pflugers Arch.* **456**, 101–115.

36. Oberhauser, A. & Carrion-Vazquez, M. (2008). Mechanical biochemistry of proteins one molecule at a time. *J. Biol. Chem.* **283**, 6617–6621.

37. Welchman, R. L., Gordon, C. & Mayer, R. J. (2005). Ubiquitin and ubiquitin-like proteins as multifunctional signals. *Nat. Rev. Mol. Cell Biol.* **6**, 599–609.

38. Hochstrasser, M. (2006). Lingering mysteries of ubiquitin-chain assembly. *Cell*, **124**, 27–34.

39. Carrion-Vazquez, M., Li, H., Lu, H., Marszalek, P., Oberhauser, A. & Fernandez, J. (2003). The mechanical stability of ubiquitin is linkage dependent. *Nat. Struct. Biol.* **10**, 738–743.

40. Pickart, C. M. & Cohen, R. E. (2004). Proteasomes and their kin: proteases in the machine age. *Nat. Rev. Mol. Cell Biol.* **5**, 177–187.

41. Chyan, C. L., Lin, F. C., Peng, H., Yuan, J. M., Chang, C. H., Lin, S. H. & Yang, G. (2004). Reversible mechanical unfolding of single ubiquitin molecules. *Biophys. J.* **87**, 3995–4006.

42. Fernandez, J. M. & Li, H. (2004). Force-clamp spectroscopy monitors the folding trajectory of a single protein. *Science*, **303**, 1674–1678.

43. Schlierf, M., Li, H. & Fernandez, J. (2004). The unfolding kinetics of ubiquitin captured with single-molecule force-clamp techniques. *Proc. Natl Acad. Sci. USA*, **101**, 7299–7304.

44. Yuan, J. M., Chyan, C. L., Zhou, H. X., Chung, T. Y., Haibo, H., Ping, G. & Yang, G. (2008). The effects of macromolecular crowding on the mechanical stability of protein molecules. *Protein Sci.* **17**, 2156–2166.

45. Cieplak, M. & Marszalek, P. (2005). Mechanical unfolding of ubiquitin molecules. *J. Chem. Phys.* **123**, 194903.

46. Grater, F. & Grubmuller, H. (2007). Fluctuations of primary ubiquitin folding intermediates in a force clamp. *J. Struct. Biol.* **157**, 557–569.

47. Imparato, A. & Pelizzola, A. (2008). Mechanical unfolding and refolding pathways of ubiquitin. *Phys. Rev. Lett.* **100**, 158104.

48. Irback, A., Mitternacht, S. & Mohanty, S. (2005). Dissecting the mechanical unfolding of ubiquitin. *Proc. Natl Acad. Sci. USA*, **102**, 13427–13432.

49. Kleiner, A. & Shakhnovich, E. (2007). The mechanical unfolding of ubiquitin through all-atom Monte Carlo simulation with a Go-type potential. *Biophys. J.* **92**, 2054–2061.

50. Li, P. C. & Makarov, D. E. (2004). Simulation of the mechanical unfolding of ubiquitin: probing different unfolding reaction coordinates by changing the pulling geometry. *J. Chem. Phys.* **121**, 4826–4832.

51. Szymczak, P. & Cieplak, M. (2006). Stretching of proteins in a force-clamp. *J. Phys. Condensed Matter*, **18**, L21.

52. West, D., Brockwell, D., Olmsted, P., Radford, S. & Paci, E. (2006). Mechanical resistance of proteins explained using simple molecular models. *Biophys. J.* **90**, 287–297.

53. Sosnick, T. R. (2004). Comment on "Force-clamp spectroscopy monitors the folding trajectory of a single protein". *Science*, **306**, 411; author reply 411.

54. Kienberger, F., Pastushenko, V. P., Kada, G., Gruber, H. J., Riener, C., Schindler, H. & Hinterdorfer, P. (2000). Static and dynamical properties of single poly (ethylene glycol) molecules investigated by force spectroscopy. *Single Mol.* **1**, 123–128.

55. Liu, Y. Z., Leuba, S. H. & Lindsay, S. M. (1999). Relationship between stiffness and force in single molecule pulling experiments. *Langmuir*, **15**, 8547–8548.

56. Forbes, J. & Wang, K. (2004). Simultaneous dynamic stiffness and extension profiles of single titin molecules: nanomechanical evidence for unfolding intermediates. *J. Vac. Sci. Technol., A*, **22**, 1439–1443.

57. Higgins, M., Sader, J. & Jarvis, S. (2006). Frequency modulation atomic force microscopy reveals individual intermediates associated with each unfolded I27 titin domain. *Biophys. J.* **90**, 640–647.

58. Janovjak, H., Muller, D. & Humphris, A. (2005). Molecular force modulation spectroscopy revealing the dynamic response of single bacteriorhodopsins. *Biophys. J.* **88**, 1423–1431.

59. Kawakami, M., Byrne, K., Brockwell, D., Radford, S. & Smith, D. (2006). Viscoelastic study of the mechanical unfolding of a protein by AFM. *Biophys. J.* **91**, L16–L18.

60. Mitsui, K., Nakajima, K., Arakawa, H., Hara, M. & Ikai, A. (2000). Dynamic measurement of single protein's mechanical properties. *Biochem. Biophys. Res. Commun.* **272**, 55–63.

61. Baker, T. & Sauer, R. (2006). ATP-dependent proteases of bacteria: recognition logic and operating principles. *Trends Biochem. Sci.* **31**, 647–653.

62. Bell, G. I. (1978). Models for the specific adhesion of cells to cells. *Science*, **200**, 618–627.

63. Evans, E. & Ritchie, K. (1997). Dynamic strength of molecular adhesion bonds. *Biophys. J.* **72**, 1541–1555.

64. Smelyanskiy, V., Dykman, M. & Golding, B. (1999). Time oscillations of escape rates in periodically driven systems. *Phys. Rev. Lett.* **82**, 3193–3197.

65. Marder, M. (1995). Fluctuations and fracture. *Phys. Rev. Lett.* **74**, 4547–4550.

66. Schlierf, M., Berkemeier, F. & Rief, M. (2007). Direct observation of active protein folding using lock-in force spectroscopy. *Biophys. J.* **93**, 3989–3998.

67. Li, P. & Makarov, D. (2004). Ubiquitin-like protein domains show high resistance to mechanical unfolding similar to that of the I27 domain in titin: evidence from simulations. *J. Phys. Chem. B*, **108**, 745–749.

68. Asbury, C. L., Fehr, A. N. & Block, S. M. (2003). Kinesin moves by an asymmetric hand-over-hand mechanism. *Science*, **302**, 2130–2134.

69. Kolomeisky, A. B. & Fisher, M. E. (2007). Molecular motors: a theorist's perspective. *Annu. Rev. Phys. Chem.* **58**, 675–695.

70. Lehmann, J., Reimann, P. & Hänggi, P. (2000). Surmounting oscillating barriers: path-integral approach for weak noise. *Phys. Rev. E: Stat. Phys., Plasmas, Fluids, Relat. Interdiscip. Top.* **62**, 6282–6303.

71. Abe, H. & Go, N. (1981). Noninteracting local-structure model of folding and unfolding transition in globular proteins. II. Application to two-dimensional lattice proteins. *Biopolymers*, **20**, 1013–1031.

72. Takada, S. (1999). Go-ing for the prediction of protein folding mechanism. *Proc. Natl Acad. Sci. USA*, **96**, 11698–11700.

73. Head-Gordon, T. & Brown, S. (2003). Minimalist models for protein folding and design. *Curr. Opin. Struct. Biol.* **13**, 160–167.

74. Oliveira, L., Schug, A. & Onuchic, J. (2008). Geometrical features of the protein folding mechanism are a robust property of the energy landscape: a detailed investigation of several reduced models. *J. Phys. Chem. B*, **112**, 6131–6136.

75. Sulkowska, J. I. & Cieplak, M. (2007). Mechanical stretching of proteins—a theoretical survey of the Protein Data Bank. *J. Phys. Condensed Matter*, **19**, 283201.

76. Block, S. M., Asbury, C. L., Shaevitz, J. W. & Lang, M. J. (2003). Probing the kinesin reaction cycle with a 2D optical force clamp. *Proc. Natl Acad. Sci. USA*, **100**, 2351–2356.

77. Maier, B., Potter, L., So, M., Long, C. D., Seifert, H. S. & Sheetz, M. P. (2002). Single pilus motor forces exceed 100 pN. *Proc. Natl Acad. Sci. USA*, **99**, 16012–16017.

78. Smith, D. E., Tans, S. J., Smith, S. B., Grimes, S., Anderson, D. L. & Bustamante, C. (2001). The bacteriophage straight phi29 portal motor can package DNA against a large internal force. *Nature*, **413**, 748–752.

79. Visscher, K., Schnitzer, M. J. & Block, S. M. (1999). Single kinesin molecules studied with a molecular force clamp. *Nature*, **400**, 184–189.

80. Yin, H., Wang, M. D., Svoboda, K., Landick, R., Block, S. M. & Gelles, J. (1995). Transcription against an applied force. *Science*, **270**, 1653–1657.

81. Best, R. B. & Hummer, G. (2005). Comment on "Force-clamp spectroscopy monitors the folding trajectory of a single protein". *Science*, **308**, 498; author reply 498.

82. Li, M., Kouza, M. & Hu, C. K. (2006). Refolding upon force quench and pathways of mechanical and thermal unfolding of ubiquitin. *Biophys. J.* **92**, 547–561.

83. Janovjak, H., Sapra, K. T., Kedrov, A. & Muller, D. J. (2008). From valleys to ridges: exploring the dynamic energy landscape of single membrane proteins. *Chem. Phys. Chem.* **9**, 954–966.

84. Kumar, S., Ma, B., Tsai, C. J., Sinha, N. & Nussinov, R. (2000). Folding and binding cascades: dynamic landscapes and population shifts. *Protein Sci.* **9**, 10–19.

85. Nevo, R., Brumfeld, V., Kapon, R., Hinterdorfer, P. & Reich, Z. (2005). Direct measurement of protein energy landscape roughness. *EMBO Rep.* **6**, 482–486.

86. Oliveberg, M. & Wolynes, P. G. (2005). The experimental survey of protein-folding energy landscapes. *Q. Rev. Biophys.* **38**, 245–288.

87. Verma, R., Peters, N. R., D'Onofrio, M., Tochtrop, G.P., Sakamoto, K. M., Varadan, R. *et al.* (2004). Ubistatins inhibit proteasome-dependent degradation by binding the ubiquitin chain. *Science*, **306**, 117–120.

88. Li, H. B., Linke, W., Oberhauser, A., Carrion-Vazquez, M., Kerkviliet, J., Lu, H. *et al.* (2002). Reverse engineering of the giant muscle protein titin. *Nature*, **418**, 998–1002.

89. Rief, M., Fernandez, J. & Gaub, H. (1998). Elastically coupled two-level systems as a model for biopolymer extensibility. *Phys. Rev. Lett.* **81**, 4764–4767.

90. Oberhauser, A., Marszalek, P., Erickson, H. & Fernandez, J. (1998). The molecular elasticity of the extracellular matrix protein tenascin. *Nature*, **393**, 181–185.

91. Vogel, V. (2006). Mechanotransduction involving multimodular proteins: converting force into biochemical signals. *Annu. Rev. Biophys. Biomol. Struct.* **35**, 459–488.

92. Evans, E. & Ritchie, K. (1999). Strength of a weak bond connecting flexible polymer chains. *Biophys. J.* **76**, 2439–2447.

93. Zinober, R. C., Brockwell, D. J., Beddard, G. S., Blake, A. W., Olmsted, P. D., Radford, S. E. & Smith, D. A. (2002). Mechanically unfolding proteins: the effect of unfolding history and the supramolecular scaffold. *Protein Sci.* **11**, 2759–2765.

94. Kedrov, A., Janovjak, H., Sapra, K. & Muller, D. (2007). Deciphering molecular interactions of native membrane proteins by single-molecule force spectroscopy. *Annu. Rev. Biophys. Biomol. Struct.* **36**, 233–260.

95. Forman, J. & Clarke, J. (2007). Mechanical unfolding of proteins: insights into biology, structure and folding. *Curr. Opin. Struct. Biol.* **17**, 58–66.

96. Cieplak, M., Hoang, T. X. & Robbins, M. O. (2004). Thermal effects in stretching of Go-like models of titin and secondary structures. *Proteins*, **56**, 285–297.

97. Tsai, J., Taylor, R., Chotchia, C. & Gerstein, M. (1999). The packing density in proteins: standard radii and volumes. *J. Mol. Biol.* **290**, 253–266.

98. Ermak, D. & McCammon, J. (1978). Brownian dynamics with hydrodynamic interactions. *J. Chem. Phys.* **69**, 1352–1360.